Theoretical Study on the Ground Resistivity Method of Electrical Prospecting

By

Takeshi KIYONO

(Received July, 1949)

1. Introduction

The resistivity of the ground can be measured by using the Wenner's electrode system (Fig. 1.1). When the current I is introduced into the ground through the outer current electrodes C_1 and C_2, and the potential difference V is measured between the two potential electrodes P_1 and P_2, the resistivity ρ of the ground can be given by the following formula:

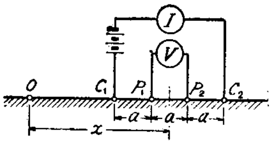

Fig. 1.1.

$$\rho=2\pi aV/I, \tag{1.1}$$

where a means the spacing of two adjacent electrodes. The above equation is valid only when the ground consists of a uniform medium, and if an orebody having different resistivity exists in the ground, the value calculated by Eq. (1.1) is not the true resistivity of the ground, but the one giving the "apparent" resistivity. This quantity generally depends on the position, direction of the electrode system and the electrode spacing.

For the Wenner configuration the apparent resistivity ρ is shown as a function of the electrode spacing a and the coordinate x of the center of the electrode system:

$$\rho=f(x, a). \tag{1.2}$$

The method in which the electrode spacing a is kept constant, moves the whole electrode system along a straight line, and the apparent resistivity ρ measured as the function of x, is called the "constant depth method", being utilized as the horizontal mapping of the buried orebody. On the contrary, the method in which the center of the system is fixed and the spacing a is variable, thereby the relation between ρ and a being obtained, is utilized in case of the vertical sounding of the geological structure.

The object of this paper is to study theoretically the resistivity curve ($\rho-x$ curve) for the constant depth profile. These curves are of use for the interpretation of practical data.

The apparent resistivity, as defined in Eq. (1.1), is obtained by multiplying the ratio of the potential difference V between the electrodes P_1 and P_2 to the current I between the electrodes C_1 and C_2 by the constant coefficient $2\pi a$. Moreover, the potential difference V can be expressed as the resultant of the four potentials by the following equation:

$$V=(V_{11}+V_{21})-(V_{12}+V_{22}), \tag{1.3}$$

where V_{ij} is the potential of the electrode P_j ($j=1;2$) due to the current electrode C_i ($i=1;2$). Therefore, the calculation of the apparent resistivity is reduced to that of the potential at any point due to a current electrode.

2. Apparent Resistivity for Linear Current Sources

It is evident that only few models can be treated accurately as three-dimensional problems, because the calculation of potential due to a point source of current is very difficult, if an orebody is buried in the ground. If we assume, however, that the current electrodes are linear electrodes of infinite length, and that the orebodies are cylindrical, which are also infinitely long and parallel to the current electrodes, then we can treat the problems as two-dimensional ones. By this approximation, the range of problems that can be solved becomes extremely wide.

In the ideal electrode system shown in Fig. 2.1, if we denote the current supplied from unit length of the energizing electrodes C_1 and C_2 by I, the potential differedce V between the potential electrodes P_1 and P_2 is given by the following equation:

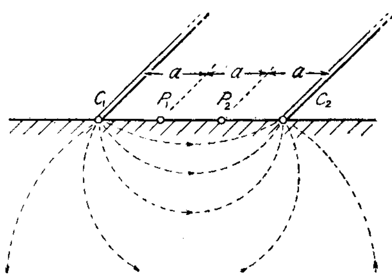

Fig. 2.1.

$$V=2\frac{\rho I}{2\pi}\log\frac{\overline{C_2P_1}\cdot\overline{C_1P_2}}{\overline{C_1P_1}\cdot\overline{C_2P_2}}, \tag{2.1}$$

where ρ means the resistivity of the medium.

For the Wenner configuration,

$$\overline{C_1P_1}=\overline{C_2P_2}=a, \qquad \overline{C_1P_2}=\overline{C_2P_1}=2a,$$

therefore, V becomes as follows:

$$V=2\frac{\rho I}{2\pi}\log 4, \tag{2.2}$$

from which the formula defining the apparent resistivity is obtained:

$$\rho=\frac{\pi}{\log 4}\frac{V}{I}. \tag{2.3}$$

It is found from the comparison of the results obtained on some simple models of orebodies, which can be treated not only as two-dimensional problems, but also as three-dimensional ones, that the two-dimensional approximation gives resistivity curves which are analogous to the actual curves properly obtained by the three-dimensional analysis. Therefore, the results obtained by the two-dimensional methods may be considered to be correct qualitatively, even when the problems could not be analysed as three-dimensional ones.

3. Application of Conformal Representation

If we adopt the two-dimensional approximation, we can apply the theory of functions of complex variables, by which the boundary of the orebody can be transformed to simpler one, and the potential can be calculated very easily. The processes of calculation of the potential using the conformal representations are as follows:

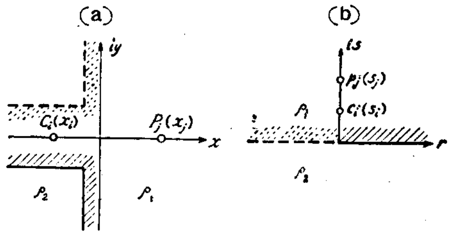

Fig. 3.1.

(i) Transform the given domain, for example Fig. 3.1 (a), into the upper half of the new plane, for example t-plane as shown in Fig. 3.1 (b), by a relation:

$$t=f(z) \quad \text{or} \quad z=\varphi(t). \tag{3.1}$$

It is convenient to choose the function $f(z)$, as it transforms the boundary of the orebody, which is assumed to be a perfect conductor or insulator, into the real axis of the t-plane (r-axis), and the ground surface (x-axis) into the imaginary axis of the t-plane (s-axis).

(ii) Obtain the relation between x and s:

$$is=f(x) \quad \text{or} \quad x=\varphi(is), \tag{3.2}$$

by which the current and potential electrodes C_i and P_j on the x-axis are transformed to the points c_i and p_j on the s-axis.

(iii) Place an electric image c_i' of the current source c_i in the r-axis, and calculate the potential at the point p_j by the following equation:

$$V_{ij} = -\frac{\rho_1 I}{\pi} \log \frac{\overline{c_i p_j}}{\overline{c_i' p_j}} \qquad \text{for} \qquad \rho_2 = 0, \tag{3.3}$$

or

$$V_{ij} = -\frac{\rho_1 I}{\pi} \log \overline{c_i p_j} \cdot \overline{c_i' p_j} \qquad \text{for} \qquad \rho_2 = \infty, \tag{3.4}$$

where

$$\overline{c_i p_j} = |\, s_i - s_j \,|, \qquad \overline{c_i' p_j} = |\, s_i + s_j \,| \tag{3.5}$$

and

$$i s_i = f(x_i), \qquad i s_j = f(x_j), \tag{3.6}$$

in which x_i and x_j mean the x-coordinates of the points C_i and P_j.

(iv) Calculate the apparent resistivity ρ by using the values of the potential V_{ij} ($i=1;2$, $j=1;2$) obtained above:

$$\left.\begin{array}{l} \rho = \dfrac{\rho}{\rho_1} = \dfrac{1}{\log 4} \displaystyle\sum_{i,j} (-)^{i+j} V_{ij}, \\ i=1;2, \qquad j=1;2. \end{array}\right\} \tag{3.7}$$

If the domain of the given plane is doubly connected, as shown in Fig. 3.2 (a), the potential must be calculated in a ring or rectangular domain (see Figs. 3.2 (b) and (c)). The processes of the calculation in this case are as follows:

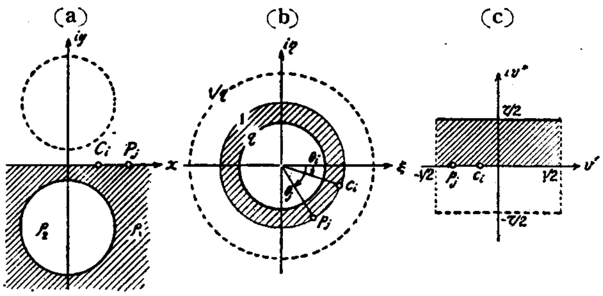

Fig. 3.2.

(i) Transform the z-plane into the ς-plane ($\varsigma = \xi + i\eta$), by a regular function:

$$\varsigma = g(z) \tag{3.8}$$

or transform into the v-plane ($v = v' + iv''$), by the relation:

$$v = \frac{1}{i2\pi} \log \varsigma. \tag{3.9}$$

It is convenient to transform the x-axis into a unit circle on the ς-plane $|\varsigma|=1$, and the boundary of the body into a circle $|\varsigma|=q<1$, and the boundary of the image body into a circle $|\varsigma|=q^{-1}>1$. These circles correspond to the real axis of the v-plane $(-\frac{1}{2}<v'<+\frac{1}{2})$, the straight lines $iv''=\tau/2$ $(-\frac{1}{2}<v'<+\frac{1}{2})$ and $iv''=-\tau/2$ $(-\frac{1}{2}<v'<+\frac{1}{2})$ respectively,
where

$$\tau=\frac{1}{i\pi}\log q \tag{3.10}$$

and

$$v'=\frac{\theta}{2\pi}, \qquad v''=-\frac{1}{2\pi}\log\rho, \tag{3.11}$$

in which

$$\varsigma=\rho e^{i\theta}. \tag{3.12}$$

(ii) Find the coordinates of the points c_i and p_j on the ς-plane or on the v-plane, which correspond to the points C_i and P_j on the x-axis.

$$\left.\begin{aligned} \rho_i&=1, & \theta_i&=\arg g(x_i),\\ \rho_j&=1, & \theta_j&=\arg g(x_j) \end{aligned}\right\} \tag{3.13}$$

or

$$\left.\begin{aligned} v_i'&=\frac{\theta_i}{2\pi}, & v_i''&=0,\\ v_j'&=\frac{\theta_i}{2\pi}, & v_j''&=0, \end{aligned}\right\} \tag{3.14}$$

(iii) Calculate the potential at p_j due to c_i by the formulae:

$$V_{ij}=-\frac{\rho_1 I}{\pi}\log\frac{\vartheta_1(v_{ij}'\,|\,2\tau)}{\vartheta_0(v_{ij}'\,|\,2\tau)}, \qquad \text{for} \qquad \rho_2=0, \tag{3.15}$$

or

$$V_{ij}=-\frac{\rho_1 I}{\pi}\log\vartheta_1(v_{ij}'\,|\,\tau), \qquad \text{for} \qquad \rho_2=\infty, \tag{3.16}$$

where

$$v_{ij}'=|v_i'-v_j'|=|\theta_i-\theta_j|/(2\pi) \tag{3.17}$$

(iv) Substitute the values of V_{ij} into Eq. (3.7) to obtain the apparent resistivity ρ.

4. Semi-infinite Horizontal Plate.

In this section, the apparent resistivity is considered for the case, where a semi-infinite plate of the perfect conductor or insulator of a thickness at_1 lies horizontally at a depth aq_1 (see Fig. 4.1).

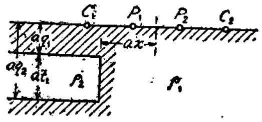

Fig. 4.1.

4.1. Theory.

The domain of the z-plane ($z=x+iy$) shown in Fig. 4.2 (a) can be transformed into the upper half of the t-plane ($t=r+is$) shown in (b) by the relation:

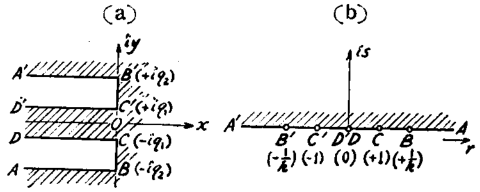

Fig. 4.2.

$$dz=C\frac{\sqrt{(1-t^2)(1-k^2t^2)}}{t}dt. \tag{4.1}$$

Integrating the above equation and determining constants, we get:

$$z=\frac{2q_1}{\pi}\left[\frac{1}{2}\sqrt{(1-k^2t^2)(1-t^2)}+\log t-\log(\sqrt{1-k^2t^2}+\sqrt{1-t^2})\right]$$

$$+\frac{2q_2}{\pi}\log(\sqrt{1-k^2t^2}+k\sqrt{1-t^2})-\frac{q_2-q_1}{\pi}\log(1-k^2)-iq_1. \tag{4.2}$$

The parameter k is determined from

$$\frac{t_1}{q_1}=\frac{q_2-q_1}{q_1}=\frac{(1-k)^2}{2k} \tag{4.3}$$

or

$$k=\frac{q_2}{q_1}-\sqrt{\left(\frac{q_2}{q_1}\right)^2-1}. \tag{4.4}$$

The relation between x and s is given by the following equation:

$$x=\frac{2q_1}{\pi}\left[\frac{1}{2}\sqrt{(1+k^2s^2)(1+s^2)}+\log s-\log(\sqrt{1+k^2s^2}+\sqrt{1+s^2})\right]$$

$$+\frac{2q_2}{\pi}\log(\sqrt{1+k^2s^2}+k\sqrt{1+s^2})-\frac{q_2-q_1}{\pi}\log(1-k^2). \tag{4.5}$$

4.2. Special Cases.

(1) $q_1\to 0$.

In the limiting case, where q_1 in Fig. 4.1 becomes zero, the following transformation must be made:

$$z=-i\frac{2t_1}{\pi}(t\sqrt{1-t^2}+\sin^{-1}t). \tag{4.6}$$

The relation between x and s is as follows:

$$x=\frac{2t_1}{\pi}\left[s\sqrt{1+s^2}+\log(s+\sqrt{1+s^2})\right]. \tag{4.7}$$

(2) $t_1 \to 0$.

From Eq. (4.3), it is found that the limit $k\to 1$ corresponds to the case $q_1=q_2$ or $t_1=0$, which represents a very thin plate. For this case, Eq. (4.2) becomes:

$$z=\frac{2q_1}{\pi}\left(\frac{1-t^2}{2}+\log t\right)-iq_1, \tag{4.8}$$

from which the relation between x and s is obtained:

$$x=\frac{2q_1}{\pi}\left(\frac{1+s^2}{2}+\log s\right). \tag{4.9}$$

(3) $t_1 \to 0$; $q_1 \to 0$.

In Fig. 4.1, if we make $t_1\to 0$ and $q_1\to 0$, a thin plate which covers the left half of the ground surface is obtained. The transformation from the z-plane to the t-plane is given by:

$$t=i\sqrt{z}. \tag{4.10}$$

Hence, s is represented as follows:

$$s=\sqrt{x} \tag{4.11}$$

(4) $t_1 \to \infty$.

In Eq. (4.3), if we make $k\to 0$, keeping $q_1\neq 0$, it becomes $q_2\to\infty$ or $t_2\to\infty$. This case corresponds to a covered vertical fault. In this limiting case Eq. (4.2) becomes as follows:

$$z=\frac{2q_1}{\pi}\left(\sqrt{1-t^2}+\log\frac{t}{1+\sqrt{1-t^2}}\right)-iq_2. \tag{4.12}$$

Hence we get the following relation between x and s:

$$x=\frac{2q_1}{\pi}\left(\sqrt{1+s^2}-\frac{1}{2}\log\frac{\sqrt{1+s^2}+1}{\sqrt{1+s^2}-1}\right). \tag{4.13}$$

4.3. Resistivity Curves.

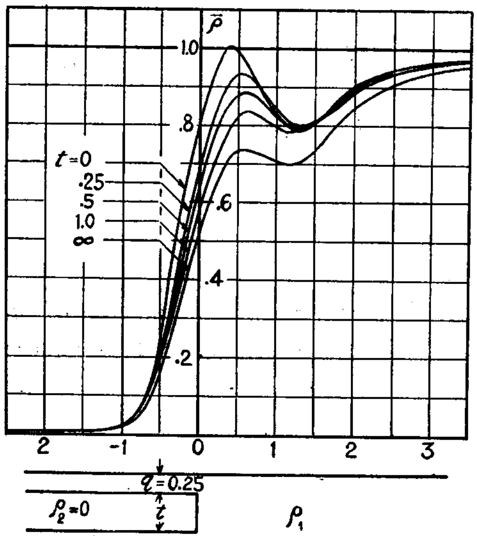

Fig. 4.3.

Fig. 4.3 shows the resistivity curves for a semi-infinite horizontal plate of the perfect conductor, the upper surface of which lies at the depth $a/4$. As the thickness of the plate increases, the maximum point of the curve is lowered, and the curve becomes flat.

Fig. 4.4 shows the curves for the insulator. It is found that the effect of the plate thickness is negligible.

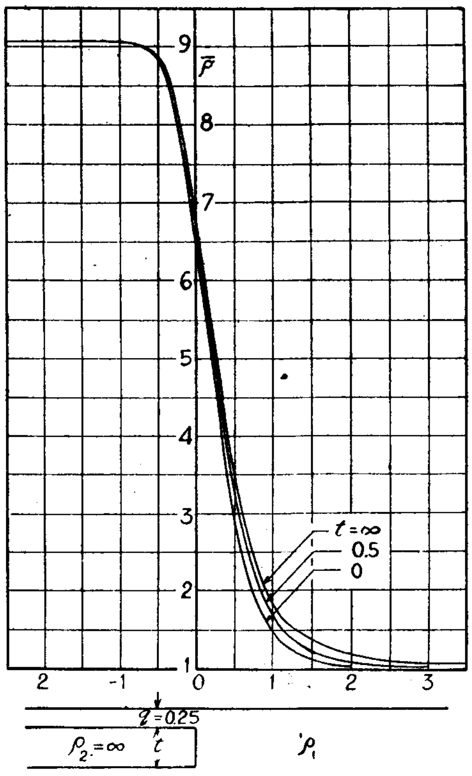

Fig. 4.4.

Fig. 4.5 shows the curves for the thin plate conductor. As the depth increases, the curves become flat.

Fig. 4.6 shows the curves for a vertical fault.

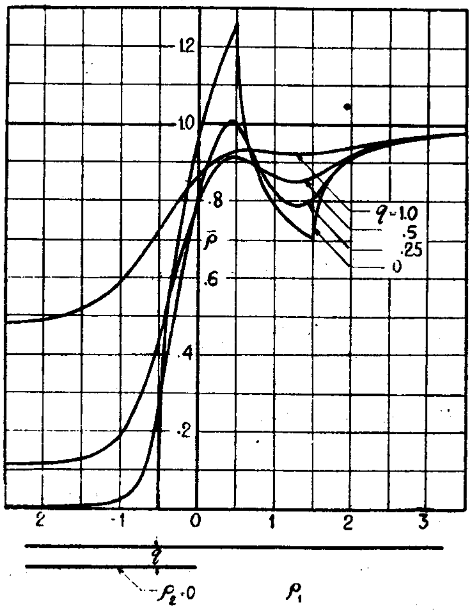

Fig. 4.5.

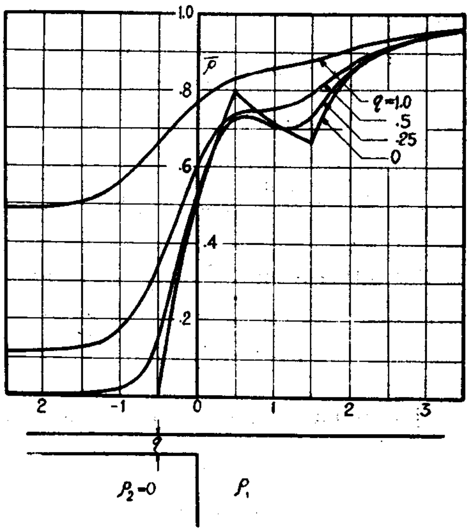

Fig. 4.6.

5. Semi-infinite Vertical Plate

In this section, the apparent resistivity curves for the semi-infinite plate of the perfect conductor or insulator with finite thickness, which is buried in a vertical position, are considered (see Fig. 5.1).

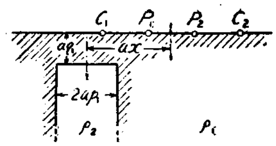

Fig. 5.1.

5.1. Theory.

The domain of the z-plane shown in Fig. 5.2 (a) can be transformed to the upper half of the t-plane (b) by the relation:

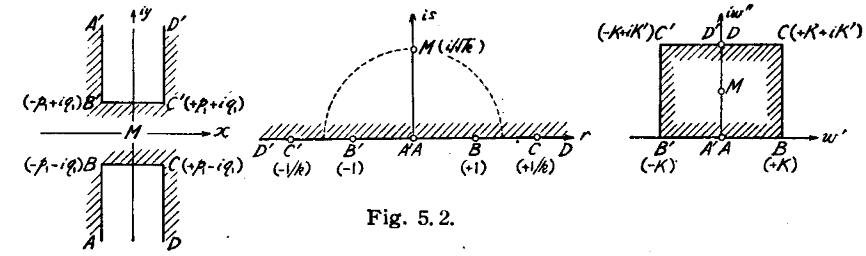

Fig. 5.2.

$$dz = C\frac{\sqrt{(1-t^2)(1-k^2t^2)}}{t^2}\,dt. \tag{5.1}$$

If we introduce a new plane shown in Fig. 5.2 (c), where $w=w'+iw''$, and put

$$t=\mathrm{sn}\,(w,k), \tag{5.2}$$

Eq. (5.1) becomes:

$$dz = C\frac{\mathrm{cn}^2\,w\cdot\mathrm{dn}^2\,w}{\mathrm{sn}^2\,w}\,dw. \tag{5.3}$$

By integrating the above equation and determining constants, we get:

$$z=\frac{i2p_1}{(1+k^2)K'-2E'}\left[k'^2w-2E(w,k)-\frac{\mathrm{cn}\,w\cdot\mathrm{dn}\,w}{\mathrm{sn}\,w}\right]-p_1. \tag{5.4}$$

The modulus k is given by the transcendental equation:

$$\frac{2p_1}{q_1}=\frac{(1+k^2)K'-2E'}{2E-k'^2K}. \tag{5.5}$$

To calculate the potential, the relation between x and s must be found. Inserting $w=iw''$ into (5.2) and (5.4), we obtain:

$$\left.\begin{aligned} x&=\frac{2p_1}{(1+k^2)K'-2E'}\Big[(1+k^2)w''-2E(w'',k')\\ &\quad+\overline{\mathrm{dn}}\,w''\left(\frac{\overline{\mathrm{sn}}\,w''}{\overline{\mathrm{cn}}\,w''}-\frac{\overline{\mathrm{cn}}\,w''}{\overline{\mathrm{sn}}\,w''}\right)\Big]-p_1;\\ s&=\frac{1}{i}\,\mathrm{sn}\,iw''=\frac{\overline{\mathrm{sn}}\,w''}{\overline{\mathrm{cn}}\,w''}, \end{aligned}\right\} \tag{5.6}$$

where $\overline{\mathrm{sn}}\,w''=\mathrm{sn}\,(w'',k')$, $\overline{\mathrm{cn}}\,w''=\mathrm{cn}\,(w'',k')$ and $\overline{\mathrm{dn}}\,w''=\mathrm{dn}\,(w'',k')$.

For numerical calculations, it is convenient to use ϑ-functions. If we put:

$$w=2Kv, \tag{5.7}$$

and represent (5.4) by ϑ-functions, we get:

$$z=\frac{iq_1}{C}\left[-2Cv-\frac{1}{2K}\frac{d}{dv}\log\vartheta_1(v,q)\vartheta_0(v,q)\right]-p_1, \tag{5.8}$$

where

$$q=e^{i\pi\tau},\qquad \tau=iK'/K, \tag{5.9}$$

and

$$\left.\begin{aligned} &C=2E-k'^2K=\frac{\pi^2}{4K}\cdot\frac{1}{G}, \\ &\frac{1}{G}=\frac{1}{3}\left[2+\vartheta_2(0)^4+\vartheta_3(0)^4\right]-16\sum_{n=1}^{\infty}\frac{nq^{2n}}{1-q^{2n}}. \end{aligned}\right\} \quad (5.10)$$

Using the above notations, Eq. (5.5) can be written as follows:

$$\frac{2p_1}{q_1}=\frac{1}{\pi}\log\frac{1}{q}-\frac{4}{\pi}G. \quad (5.11)$$

The parameter q of ϑ-functions can be determined by the above equation.

The relation between x and s is given by the following equations:

$$\left.\begin{aligned} &x=\frac{q_1}{C}\left[2Cv''-\frac{1}{2K}\cdot\frac{i\vartheta_1'(iv'',\sqrt{q})}{\vartheta_1(iv'',\sqrt{q})}\right]-p_1, \\ &s=\frac{\vartheta_3(0,q)}{\vartheta_2(0,q)}\cdot\frac{\vartheta_1(iv'',q)}{i\vartheta_9(iv'',q)}. \end{aligned}\right\} \quad (5.12)$$

If we develop the ϑ-functions into series, we get the following equations:

$$x=\frac{2q_1}{\pi}\left[\pi v''-\frac{\pi^2}{4KC}\cdot\frac{\cosh\pi v''-3q\cosh 3\pi v''+5q^3\cosh 5\pi v''-\cdots}{\sinh\pi v''-q\sinh 3\pi v''+q^3\sinh 5\pi v''-\cdots}\right]-p_1,$$

$$s=2q^{1/4}\frac{\vartheta_3}{\vartheta_2}\cdot\frac{\sinh\pi v''-q^2\sinh 3\pi v''+q^6\sinh 5\pi v''-\cdots}{1-2q\cosh 2\pi v''+2q^4\cosh 4\pi v''-\cdots}. \quad (5.13)$$

It is found that the point $z=0$ corresponds to $t=i/\sqrt{k}$, $w=iK'/2$ and $v=\tau/2$. It should be noted that

$$s(-x)=\frac{1}{k}\cdot\frac{1}{s(+x)}. \quad (5.14)$$

In the case, where the parameter q is very small, the following approximate formulae can be used:

$$\left.\begin{aligned} &x=\frac{2q_1}{\pi}(w''-\coth w'')-p_1, \\ &K'=2+\pi\frac{p_1}{q_1}; \\ &s=\sinh w'' \quad \text{for} \quad w''<K'/2. \end{aligned}\right\} \quad (5.15)$$

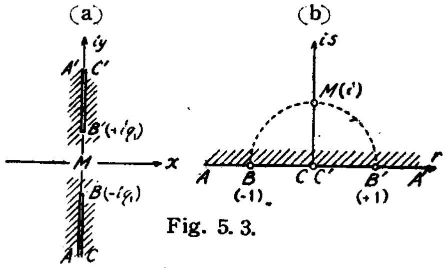

Fig. 5. 3.

5. 2. Special Case.

The limiting case, when the modulus k becomes unity, corresponds to a vertical plate of zero thickness. Then Eqs. (5.4) and (5.2) are written as follows:

$$\left.\begin{aligned} z&=-iq_1\coth 2w, \\ t&=\tanh w, \end{aligned}\right\} \tag{5.16}$$

from which we get:

$$z=-\frac{iq_1}{2}\frac{1+t^2}{t} \tag{5.17}$$

(see Fig. 5. 3). Hence

$$x=\frac{q_1}{2}\left(s-\frac{1}{s}\right), \tag{5.18}$$

or

$$s=\frac{x}{q_1}+\sqrt{\left(\frac{x}{q_1}\right)^2+1}. \tag{5.19}$$

5. 3. Resistivity Curves.

In Fig. 5. 4, the curves for perfect conductor are shown, in which the depth q is kept constant, and the breadth $2p$ is taken as parameter. When the breadth is large, the curve is vUv-shaped, and when the breadth is equal to the electrode spacing, that is $2p=1$, the vVv-curve is obtained.

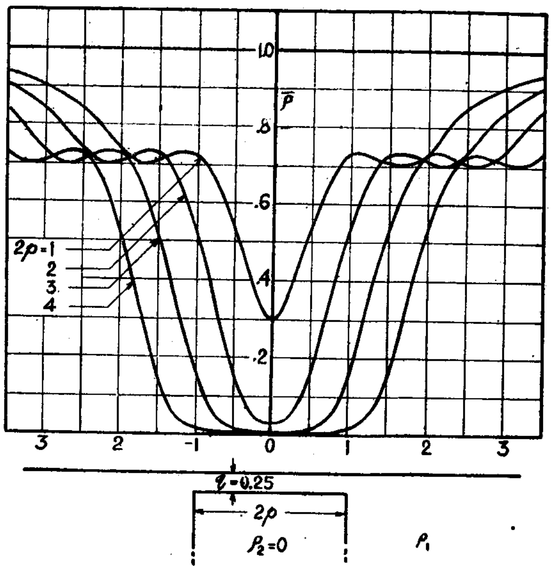

Fig. 5. 4.

Fig. 5.5 shows the curves, when the breadth is smaller than the electrode spacing ($2p<1$). The form of the curves varies from vVv to W, as the beradth decreases.

In Fig. 5.6, the breadth $2p$ is kept constant, and the depth q is varied. With increasing depth, the curves become flat. Fig. 5.7 shows the curves for a very thin plate (W-curves).

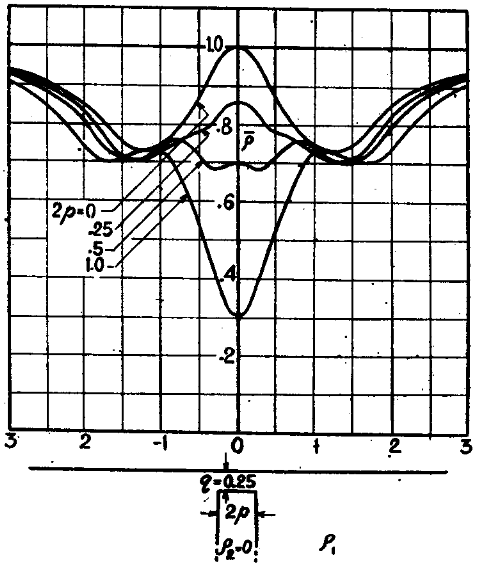

Fig. 5.5.

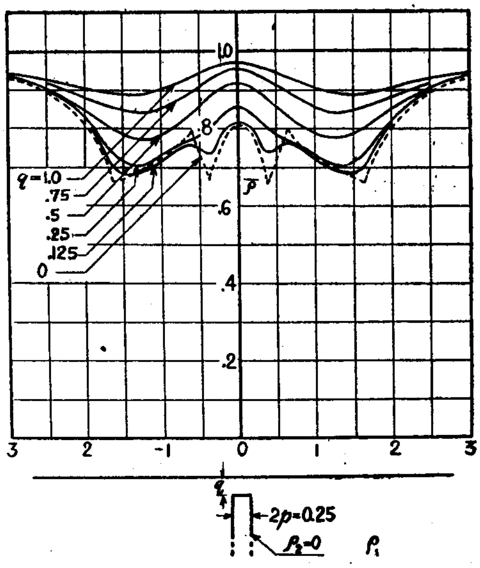

Fig. 5.6.

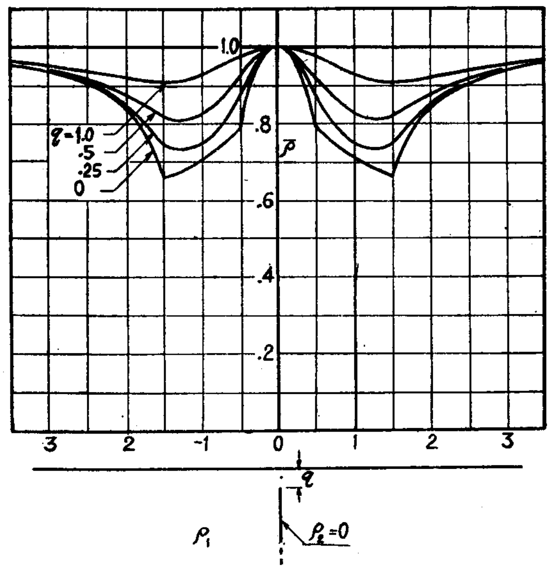

Fig. 5.7.

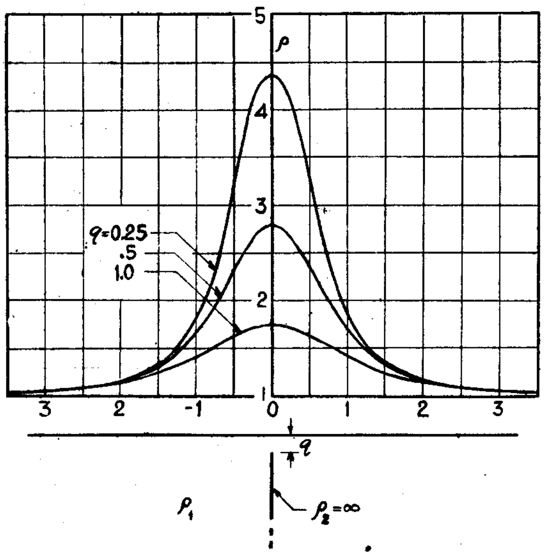

Fig. 5.8.

Fig. 5.8 shows the curves for a very thin plate of insulator. They are inverted V-shaped. It is found that the maximum point of the curve is lowered, when the depth is increased.

6. Thin Vertical Plate

In this section, the apparent resistivity for a thin vertical plate as shown in Fig. 6.1 is considered.

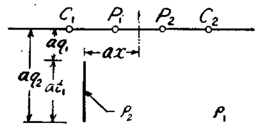

Fig. 6.1.

6.1. Theory.

The domain ABDFG shown in Fig. 6.2 (a) can be transformed into the t-plane shown in (b) by the relation:

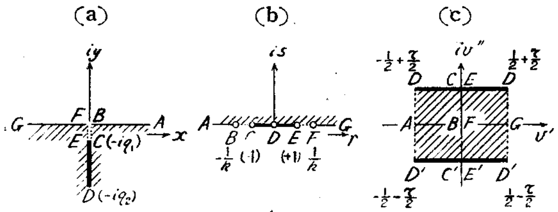

Fig. 6.2.

$$dz = C\frac{t}{\sqrt{1-k^2t^2}}\,dt. \tag{6.1}$$

Integrating the above equation, we obtain:

$$z = -iq_2\sqrt{1-k^2t^2}, \tag{6.2}$$

where

$$\sqrt{1-k^2} = k' = q_1/q_2. \tag{6.3}$$

To calculate the potential, we must transform the t-plane into the rectangular domain of the v-plane shown in Fig. 6.2 (c), by means of the following relation:

$$t = \mathrm{sn}\,(K + iK' - 2Kv, k)$$

$$= \frac{1}{k} \frac{\mathrm{dn}\,2Kv}{\mathrm{cn}\,2Kv}, \tag{6.4}$$

or

$$z = -q_1 \frac{\mathrm{sn}\,(2Kv, k)}{\mathrm{cn}\,(2Kv, k)}, \tag{6.5}$$

or

$$z = -q_1 \frac{\vartheta_3}{\vartheta_0} \cdot \frac{\vartheta_1(v \mid \tau)}{\vartheta_2(v \mid \tau)}. \tag{6.6}$$

The relation between x and v' is as follows:

$$x = -q_1 \frac{\mathrm{sn}\,2Kv'}{\mathrm{cn}\,2Kv'}$$

$$= -q_1 \frac{\vartheta_3}{\vartheta_0} \cdot \frac{\vartheta_1(v')}{\vartheta_2(v')}. \tag{6.7}$$

The potential at any point P on the x-axis due to a current source C on the x-axis, can be calculated by the formula (3.15) or (3.16).

6.2. Numerical Calculation.

In most cases, the modulus $k \fallingdotseq 1$, and consequently, the parameter $q \fallingdotseq 1$. So we apply the Jacobi's transformation to Eq. (6.7), and write:

$$x = -q_1 \frac{\vartheta_3(0 \mid \tau')}{\vartheta_2(0 \mid \tau')} \cdot \frac{i\vartheta_1\left(\frac{v'}{\tau} \middle| \tau'\right)}{\vartheta_0\left(\frac{v'}{\tau} \middle| \tau'\right)}, \tag{6.8}$$

where

$$\tau' = -1/\tau = iK/K'. \tag{6.9}$$

By developing the ϑ-functions into q-series, it becomes as follows:

$$x = -q_1 Q \frac{\sinh \xi - q'^2 \sinh 3\xi + q'^6 \sinh 5\xi - \cdots}{1 - 2q' \cosh 2\xi + 2q'^4 \cosh 4\xi - \cdots}, \tag{6.10}$$

where

$$Q = 2q'^{1/4} \frac{\vartheta_3(0 \mid \tau')}{\vartheta_2(0 \mid \tau')} = \frac{1 + 2q' + 2q'^4 + \cdots}{1 + q'^2 + q'^6 + \cdots}, \tag{6.11}$$

$$\xi = i\pi v'/\tau = \pi K v'/K', \tag{6.12}$$

and

$$\left. \begin{aligned} q' &= \varepsilon' + 2\varepsilon'^5 + 15\varepsilon'^9 + \cdots, \\ \varepsilon' &= (1/2)\cdot(1-\sqrt{k})/(1+\sqrt{k}). \end{aligned} \right\} \tag{6.13}$$

For larger values of variable ξ, we use the following relations:

$$x = -q_1 \frac{\vartheta_3(0\ \tau')}{\vartheta_2(0\ \tau')} \cdot \frac{\vartheta_0(\bar{v}'/\tau\ \tau')}{i\vartheta_1(\bar{v}'/\tau\ \tau')}, \tag{6.14}$$

or

$$x = -q_1 \frac{Q}{4\sqrt{q'}} \cdot \frac{1 - 2q' \cosh 2\eta + 2q'^4 \cosh 4\eta - \cdots}{\sinh \eta - q'^2 \sinh 3\eta + q'^6 \sinh 5\eta - \cdots}, \tag{6.15}$$

where

$$\bar{v}' = \frac{1}{2} - v'; \qquad \eta = \frac{\pi}{2}\frac{K}{K'} - \xi. \tag{6.16}$$

6.3. Special Case.

If the depth q_1 in Fig. 6.1 is reduced to zero, the z-plane becomes as shown in Fig. 6.3 (a). This can be transformed to the upper half of the t-plane (b), by means of the relation:

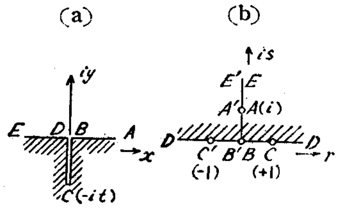

Fig. 6.3.

$$z = -i2t_1 \frac{t}{1+t^2}. \tag{6.17}$$

from which we obtain:

$$x = 2t_1 \frac{s}{1-s^2}, \tag{6.18}$$

or

$$s = \frac{t_1}{x} + \sqrt{\left(\frac{t_1}{x}\right)^2 + 1}. \tag{6.19}$$

6.4. Resistivity Curves.

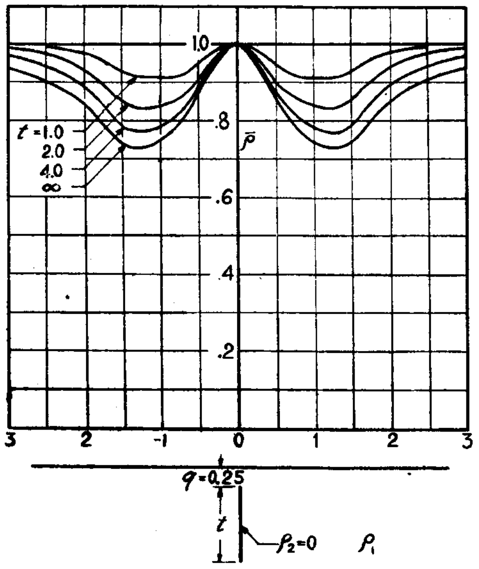

Fig. 6.4.

Figs. 6.4 and 6.5 show the curves for the plates of finite depths. In both cases, the curves are W-shaped, which are similar to the curves shown in Fig. 5.7.

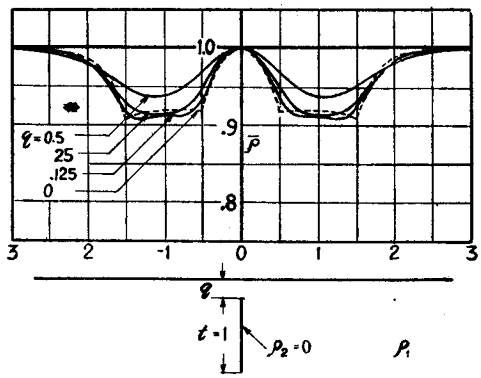

Fig. 6.5.

Fig. 6.6 shows the curves for the non-conducting plates of zero depth.

In Fig. 6.7, the curves are shown for a plate of the insulator. In mcst cases, they are inverted vVv-shaped.

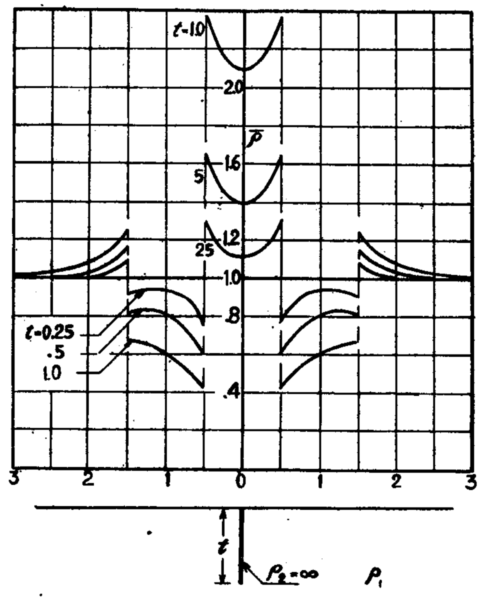

Fig. 6.6.

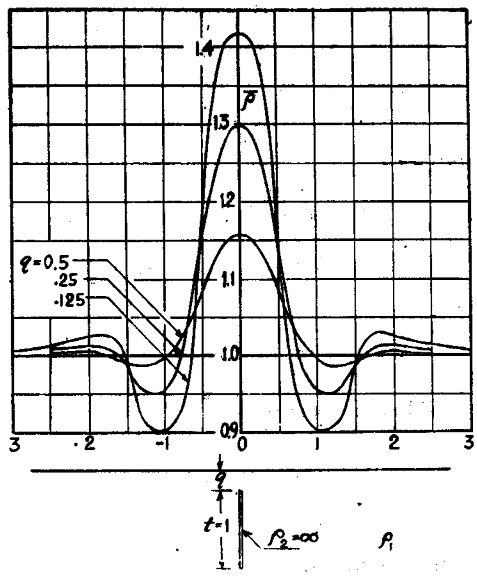

Fig. 6.7.

7. Thin Horizontal Plate

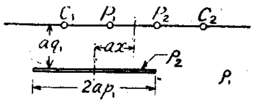

Fig. 7.1.

In this section, a thin plate of finite depth buried in a horizontal position, is considered (see Fig. 7.1).

7.1. Theory.

The domain ABC$\cdots$GH shown in Fig. 7.2 (a) can be transformed to the t-plane (b) by the relation:

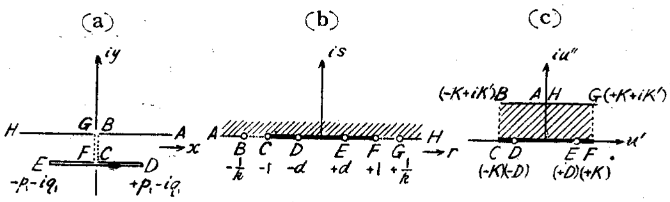

Fig. 7.2.

$$dz = C\frac{t^2-d^2}{\sqrt{(1-t^2)(1-k^2t^2)}}\,dt. \tag{7.1}$$

Substituting

$$t = \mathrm{sn}\,(u, k) \tag{7.2}$$

into Eq. (7.1), and integrating, we get:

$$z = \frac{2q_1}{\pi}\left[E\cdot u - K\cdot E(u,k)\right] - iq_1, \tag{7.3}$$

where

$$\left.\begin{aligned} \frac{p_1}{q_1} &= \frac{2}{\pi}\left[K\cdot E(D,k) - E\cdot D\right], \\ k^2d^2 &= 1-\frac{E}{K} \end{aligned}\right\} \tag{7.4}$$

and

$$d = \mathrm{sn}\,(D, k). \tag{7.5}$$

To transform the domain of Fig. 7.2 (c) into the v-plane shown in Fig. 3.2, we put:

$$u = \pm K + iK' - 2Kv. \tag{7.6}$$

Then it becomes:

$$z = \frac{2q_1}{\pi}\left[K\cdot E(2Kv,k) - E\cdot 2Kv - K\frac{\mathrm{sn}\,2Kv\cdot \mathrm{dn}\,2Kv}{\mathrm{cn}\,2Kv}\right], \tag{7.7}$$

from which we obtain the following relation:

$$x=\frac{2q_1}{\pi}\left[K\cdot E(2Kv', k)-E\cdot 2Kv-K\frac{\operatorname{sn}2Kv'\cdot\operatorname{dn}2Kv'}{\operatorname{cn}2Kv'}\right], \tag{7.8}$$

or

$$x=\frac{2q_1}{\pi}\left[E\cdot 2K\bar{v}'-K\cdot E(2K\bar{v}', k)-K\frac{\operatorname{cn}2K\bar{v}'\cdot\operatorname{dn}2K\bar{v}'}{\operatorname{sn}2K\bar{v}'}\right], \tag{7.9}$$

where

$$\bar{v}'=\frac{1}{2}-v'. \tag{7.10}$$

The potential is calculated by means of the formulae (3.15) or (3.16).

9.2. Numerical Calculation.

If we use the ϑ-function, (7.7) can be represented as follows:

$$z=\frac{q_1}{\pi}\cdot\frac{d}{dv}\log\vartheta_2(v\ \ \tau), \tag{7.11}$$

hence it becomes:

$$x=\frac{q_1}{\pi}\cdot\frac{d}{dv'}\log\vartheta_2(v'\ \ \tau), \tag{7.12}$$

or by means of the Jacobi's transformation:

$$x=\frac{2q_1}{\pi}\left(-\frac{i\pi}{\tau}v'+\frac{1}{2\tau}\cdot\frac{\vartheta_0'\left(\frac{v'}{\tau}\middle|\tau'\right)}{\vartheta_0\left(\frac{v'}{\tau}\middle|\tau'\right)}\right), \tag{7.13}$$

where

$$\tau'=-1/\tau. \tag{7.14}$$

Developing the ϑ-function, we get:

$$x=-\frac{2q_1}{\pi}\left(\xi+2\xi_m\frac{2q'\sinh 2\xi-4q'^4\sinh 4\xi+\cdots}{1-2q'\cosh 2\xi+2q'^4\cosh 4\xi-\cdots}\right), \tag{7.15}$$

where

$$\xi=\frac{i\pi}{\tau}v'=\pi\frac{K}{K'}v', \qquad \xi_m=\frac{i\pi}{\tau}\frac{1}{2}=-\frac{1}{2}\log q'. \tag{7.16}$$

When ξ approaches its maximum value ξ_m, the other formula should be used. Inserting (7.10) into (7.12), we obtain:

$$x=-\frac{q_1}{\pi}\cdot\frac{d}{d\bar{v}'}\log\vartheta_1(\bar{v}'\,|\,\tau). \tag{7.17}$$

Then, by Jabobi's transformation, it becomes:

$$x=-\frac{q_1}{\pi}\left(-2\frac{i\pi}{\tau}\bar{v}'+\frac{1}{\tau}\cdot\frac{\vartheta_1'\left(\frac{v'}{\tau}\middle|\tau'\right)}{\vartheta_1\left(\frac{v'}{\tau}\middle|\tau'\right)}\right), \tag{7.18}$$

from which the following formula is obtained:

$$x=\frac{2q_1}{\pi}\left(\eta-2\xi_m\frac{\cosh\eta-3q'^2\cosh 3\eta+5q'^6\cosh 5\eta-\cdots}{\sinh\eta-q'^2\sinh 3\eta+q'^6\sinh 5\eta-\cdots}\right), \tag{7.19}$$

where

$$\eta=\xi_m-\xi. \tag{7.20}$$

If we represent (7.4) by means of the ϑ-functions, the following equations are obtained:

$$\left.\begin{aligned}&\frac{p_1}{q_1}=\frac{2}{\pi}\left[\frac{1}{2\tau}\cdot\frac{\vartheta_2'\left(\frac{v_a}{\tau}\middle|\tau'\right)}{\vartheta_2\left(\frac{v_a}{\tau}\middle|\tau'\right)}-\frac{i\pi}{\tau}v_a\right],\\&\frac{\vartheta_2''\left(\frac{v_a}{\tau}\middle|\tau'\right)}{\vartheta_2\left(\frac{v_a}{\tau}\middle|\tau'\right)}-\frac{\vartheta_2'\left(\frac{v_a}{\tau}\middle|\tau'\right)^2}{\vartheta_2\left(\frac{v_a}{\tau}\middle|\tau'\right)^2}=i2\pi\tau,\end{aligned}\right\} \tag{7.21}$$

where

$$v_a=D/(2K). \tag{7.22}$$

When the value of the parameter $q'=\exp(-i\pi/\tau)$ is very small, the constants ξ_m or K can be calculated by means of the approximate formula:

$$\frac{p_1}{q_1}=\frac{2}{\pi}\left(\sqrt{\xi_m(\xi_m-1)}-\tanh^{-1}\sqrt{\frac{\xi_m-1}{\xi_m}}\right). \tag{7.23}$$

In such a case

$$K\simeq\xi_m. \tag{7.23'}$$

7.3. Special Case.

For the limiting case $q_1 \to 0$, we can transform the z-plane, Fig. 7.3 (a), into the t-plane (b), by the following equation:

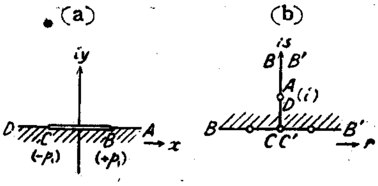

Fig. 7.3.

$$-z = p_1 \frac{1-t^2}{1+t^2}. \tag{7.24}$$

The relation between x and s becomes as follows:

$$s = \sqrt{\frac{x+p_1}{x-p_1}}, \qquad |x| > p_1. \tag{7.25}$$

In this case, the potential can be calculated by Eq. (3.3) or (3.4).

7.4. Resistivity Curves.

The resistivity curves for conducting plates of zero depth are shown in Fig. 7.4. When the breadth $2ap$ is larger than the electrode spacing a, the curves are vVv- or vUv-shaped, and in the case $2p<1$, a maximum appears at the center of the plate.

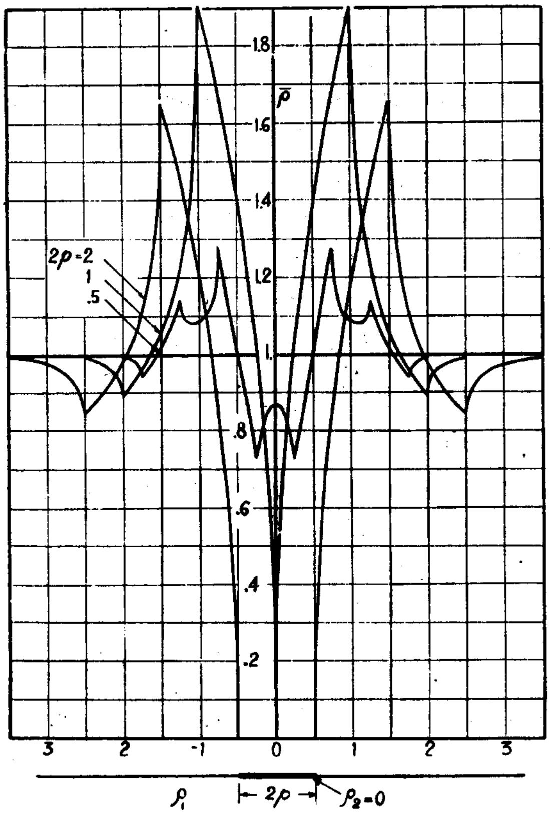

Fig. 7.4.

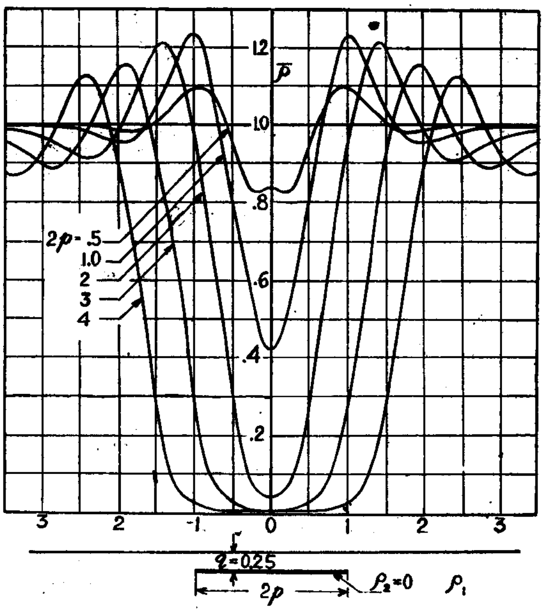

Fig. 7.5.

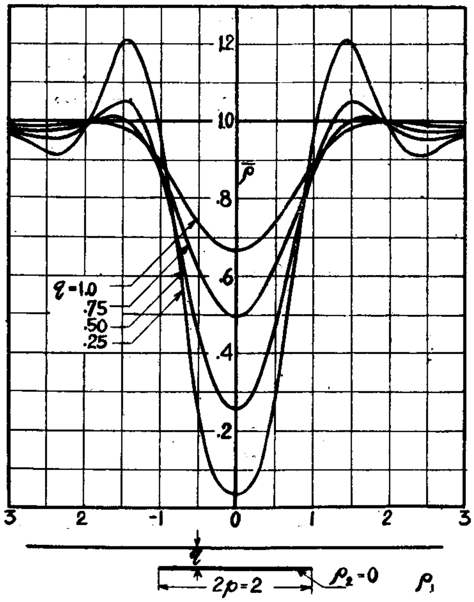

Fig. 7.6.

Fig. 7.5 shows the curves for finite depth. The type of these curves is similar to those of zero depth.

In Fig. 9.6, are shown the curves for perfect conductor, taking the depth q as parameter. It is found that the vVv- or vUv-curves reduce to V- or U-curves with increasing depth.

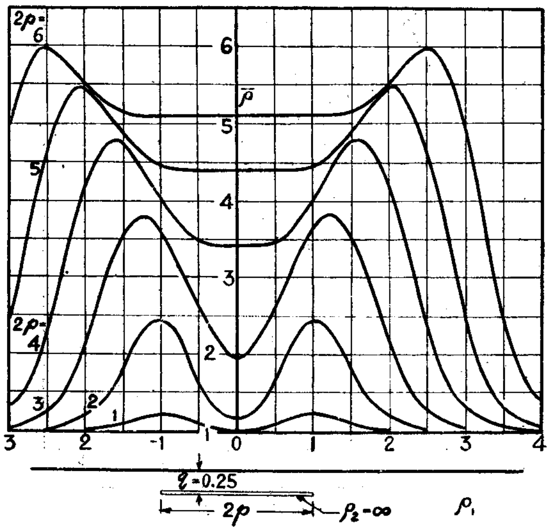

Fig. 7.7.

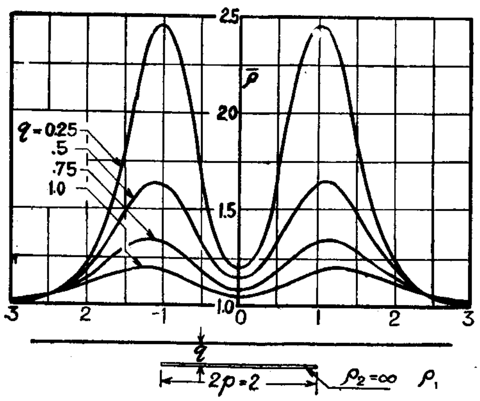

Fig. 7.8.

Fig. 7.7 shows the curves for the non-conducting plate of a constant depth, taking the breadth $2p$ as parameter. They are inverted W-shaped, and approach the inverted U-curves with increasing breadth. In Fig. 7.8, are shown the curves for various values of the depth and a constant breadth $2p=2$.

These results are summarized in the following table, combining with those obtained in the section 6:

	Conductor	Non-conductor
Vertical	W	inverted vVv
Horizontal	vVv	inverted W

8. Circular Cylinder

We calculate the apparent resistivity for a buried cylinder with circular section, as shown in Fig. 8.1. The resistivity of the cylinder ρ_2 is assumed to be zero or infinity.

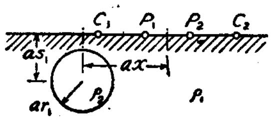

Fig. 8.1.

8.1. Theory.

The domain of the z-plane shown in Fig. 8.2 (a) can be transformed to a ring domain of the ς-plane (b) by the linear transformation:

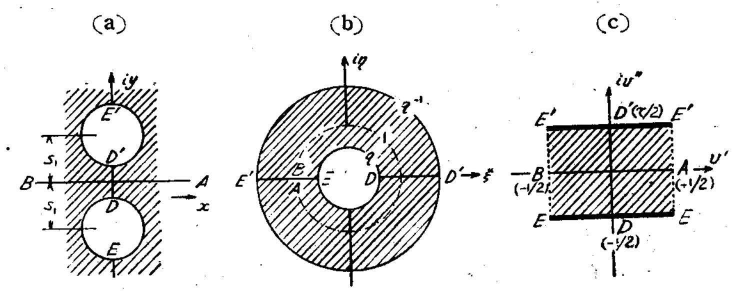

Fig. 8.2.

$$z=it_1\frac{1-\varsigma}{1+\varsigma}, \tag{8.1}$$

where

$$t_1=\sqrt{s_1^2-r_1^2}. \tag{8.2}$$

The x-axis corresponds to the unit circle:

$$\varsigma = e^{i\theta}, \tag{8.3}$$

and the relation between x and θ is given by:

$$\theta=2\tan^{-1}\frac{x}{t_1}. \tag{8.4}$$

To calculate the potential, we must transform the ς-plane to the v-plane shown in Fig. 3.2 or in Fig. 8.2 (c), by the relation:

$$v=\frac{1}{i2\pi}\log\varsigma \tag{8.5}$$

or

$$v'=\frac{\theta}{2\pi}, \qquad v''=-\frac{1}{2\pi}\log\rho, \tag{8.6}$$

where

$$v=v'+iv'', \qquad \varsigma=\rho e^{i\theta}. \tag{8.7}$$

8.2. Resistivity Curves.

Fig. 8.3 shows the curves for a cylindrical conductor, the diameter of which is equal to the electrode spacing a. As the depth increases, vVv-curves are reduced to V-curves.

Fig. 8.4 shows the curves for a non-conducting circular cylinder. They are similar to the curves for a vertical plate (see Fig. 6.7).

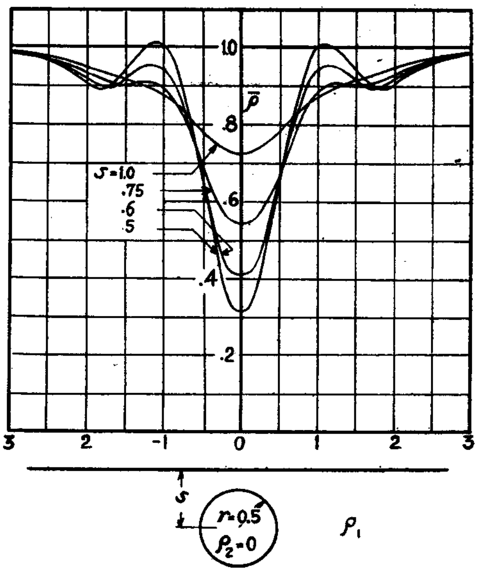

Fig. 8.3.

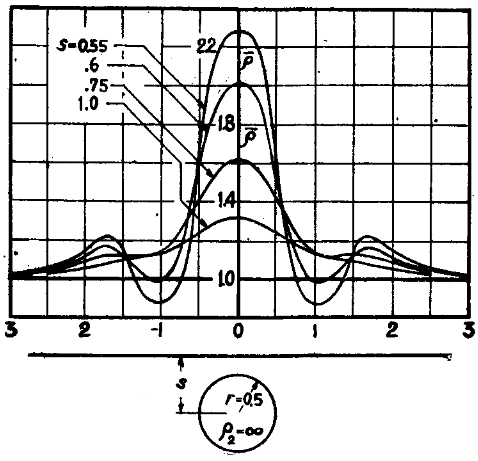

Fig. 8.4.

9. Circular Cylinder of Finite Conductivity

9.1. Theory.

We can also calculate the potential in the case, where the resistivity ρ_2 of the buried cylinder shown in Fig. 8.1 is finite. In this case, the following formula must be used for the calculation:

$$V_{ij} = -\frac{\rho_1 I}{\pi} \log \sin \pi v_{ij}' - \frac{\rho_1 I}{\pi} \sum_{m=1}^{\infty} h^m \log(1 - \operatorname{sech} 2\pi m\kappa \cdot \cos 2\pi v_{ij}'), \tag{9.1}$$

where

$$v_{ij}' = |v_i' - v_j'|, \qquad \kappa = \tau / i \tag{9.2}$$

and

$$h = (\rho_2 - \rho_1)/(\rho_2 + \rho_1). \tag{9.3}$$

9.2. Resistivity Curves.

Figs. 9.1 and 9.2 show the curves for the cylinders of finite conductivity. It is found that the curves for the good conductor ($\rho_2 < \rho_1$) are similar to those of the perfect conductor ($\rho_2 = 0$), and the curves for the poor conductor ($\rho_2 > \rho_1$) to those of the insulator ($\rho_2 = \infty$).

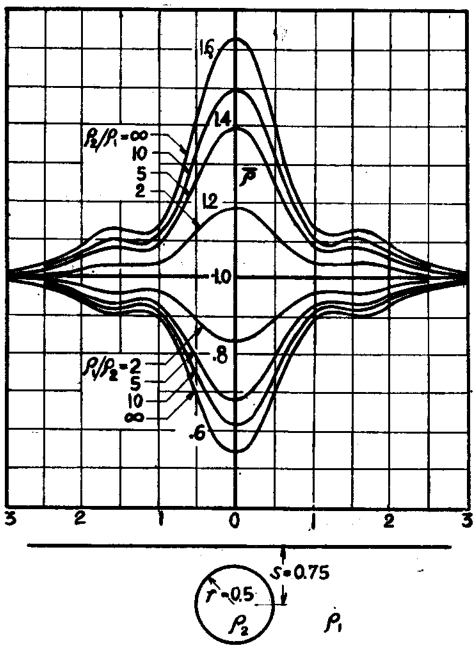

Fig. 9.1.

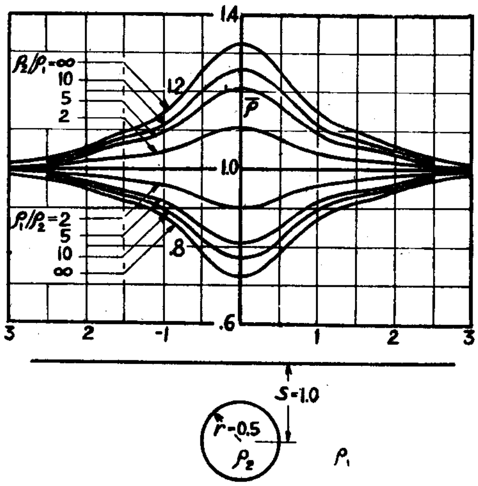

Fig. 9.2.

10. Antieline

We consider the potential due to a symmetrical anticline as shown in Fig. 10.1. It is assumed that the two inclined planes intersect to each other at right angle.

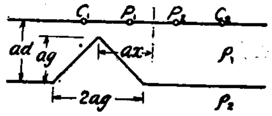

Fig. 10.1.

10. 1. Theory.

To calculate the potential, we must transform the domain of the z-plane, Fig. 10.2 (a), into the upper half of the t-plane (b). It is convenient, however, to introduce an auxiliary plane ς, Fig. 10.2 (c). The transformation from z to ς is given by the following equation:

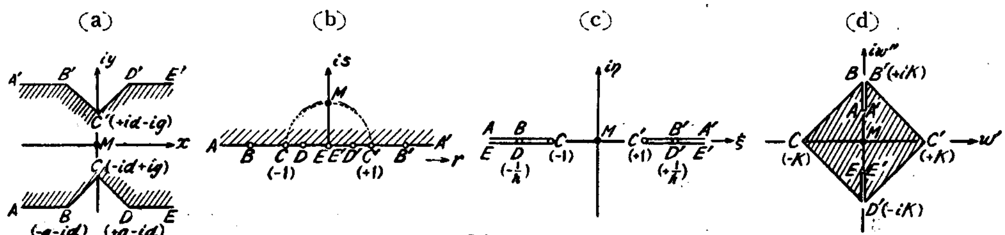

Fig. 10.2.

$$dz=C(\varsigma^2-1)^{-1/4}\left(\varsigma^2-\frac{1}{h^2}\right)^{-1/4}d\varsigma. \tag{10.1}$$

To integrate the above equation, we put:

$$\varsigma^2=\frac{1-\operatorname{cn}^4(w,k)}{1-h^2\operatorname{cn}^4(w,k)}, \qquad k=1/\sqrt{2}\,. \tag{10.2}$$

The domain of the w-plane is shown in Fig. 10.2 (d). The relation between ς and t is given by:

$$\varsigma=\frac{1}{2}\,\frac{1+t^2}{t}\,. \tag{10.3}$$

Inserting (10.2) into (10.1) and integrating, we get:

$$z=C\sqrt{2}\,\frac{\operatorname{dn}\alpha}{\operatorname{sn}\alpha}\left[\frac{\operatorname{sn}\alpha\cdot\operatorname{dn}\alpha}{\operatorname{cn}\alpha}\,w-\Pi(w,\alpha)+i\Pi(w,i\alpha)\right], \tag{10.4}$$

where

$$h=\frac{1}{2}\,\frac{\operatorname{sn}^2(\alpha,k)}{\operatorname{dn}^2(\alpha,k)}, \qquad k=1/\sqrt{2}\,. \tag{10.5}$$

If we represent the Π-function by the ϑ-function, Eq. (10.4) becomes as follows:

$$z=i\frac{2d}{\pi}\left[2\pi cv-\frac{1}{2}\log\frac{\vartheta_0(v-c\,|\,\tau)}{\vartheta_0(v+c\,|\,\tau)}+\frac{i}{2}\log\frac{\vartheta_0(v-ic\,|\,\tau)}{\vartheta_0(v+ic\,|\,\tau)}\right] \quad (10.6)$$

where

$$w=2Kv, \qquad \tau=i$$

and

$$c=(d-g)/(2d). \quad (10.7)$$

The relation between x and v'' is given by:

$$x=-\frac{2d}{\pi}\left[\psi(v'',c)+\varphi(v'',c)\right], \quad (10.8)$$

where

$$\left.\begin{aligned}\psi(v'',c)&=\frac{1}{2}\log\frac{\vartheta_2(v''-c)}{\vartheta_2(v''+c)},\\ \varphi(v'',c)&=\sum_{n=1}^{\infty}\tan^{-1}\frac{\sin 2\pi c\cdot\sinh 2\pi v''}{\cosh(2n-1)\pi-\cos 2\pi c\cdot\cosh 2\pi v''}\end{aligned}\right\} \quad (10.9)$$

The value of s which corresponds to v'', can be calculated as follows:

$$\left.\begin{aligned}\eta&=\sqrt{2}\,\frac{\operatorname{sn}2Kv''\cdot\operatorname{dn}2Kv''}{\sqrt{\operatorname{cn}^4 2Kv''-h^2}},\\ s&=\sqrt{1+\eta^2}+\eta.\end{aligned}\right\} \quad (10.10)$$

10.2. Numerical Calculation:

Eq. (10.8) can be written as follows:

$$-x=d\left[L(\chi,\gamma)+T(\chi,\gamma)\right], \quad (10.11)$$

where

$$L(\chi,\gamma)=\frac{1}{\pi}\left[\log\frac{\cos(\chi-\gamma)}{\cos(\chi+\gamma)}+\sum_{n=1}^{\infty}\log\frac{1+q^{4n}+2q^{2n}\cos 2(\chi-\gamma)}{1+q^{4n}+2q^{2n}\cos 2(\chi+\gamma)}\right], \quad (10.12)$$

or

$$L(\chi,\gamma)=\frac{1}{\pi}\log\frac{(c_1\cos\chi+c_3\cos 3\chi+\cdots)+(s_1\sin\chi+s_3\sin 3\chi+\cdots)}{(c_1\cos\chi+c_3\cos 3\chi+\cdots)-(s_1\sin\chi+s_3\sin 3\chi+\cdots)}, \quad (10.13)$$

in which

$$\left.\begin{array}{lll} c_1=\cos\gamma, & c_3=q^2\cos 3\gamma, & c_3=q^6\cos 5\gamma,\cdots; \\ s_1=\sin\gamma, & s_3=q^2\sin 3\gamma, & s_5=q^6\sin 5\gamma,\cdots, \end{array}\right\} \tag{10.14}$$

and

$$T(\chi,\gamma)=\frac{2}{\pi}\sum_{n=1}^{\infty}\tan^{-1}\frac{\sin 2\gamma\cdot\sinh 2x}{\cosh(2n-1)\pi-\cos 2\gamma\cdot\cosh 2\chi}, \tag{10.15}$$

and

$$\chi=\pi v''=\frac{\pi}{2K}w'', \qquad \gamma=\pi c=\frac{\pi}{2K}u. \tag{10.16}$$

If we write:

$$Y=1+\frac{1}{\eta^2}=H[1+F(\chi)], \tag{10.17}$$

the values of s can be calculated from the following relations:

$$\left.\begin{array}{ll} s=(\sqrt{Y}-1)/\sqrt{Y-1}, & \text{for} \quad x>0; \\ s=\sqrt{Y-1}/\sqrt{(Y-1)}, & \text{for} \quad x<0, \end{array}\right\} \tag{10.18}$$

where

$$\frac{1}{H}=1+2^{3/4}\frac{\vartheta_3\left(\frac{2\gamma}{\pi}\right)}{\vartheta_0\left(\frac{2\gamma}{\pi}\right)+\vartheta_2\left(\frac{2\gamma}{\pi}\right)}, \tag{10.19}$$

and

$$F(\chi)=2^{3/4}\frac{\vartheta_3\left(\frac{2\chi}{\pi}\right)}{\vartheta_0\left(\frac{2\chi}{\pi}\right)-\vartheta_2\left(\frac{2\chi}{\pi}\right)}. \tag{10.20}$$

10.3. Resistivity Curves.

Fig. 10.3 shows the resistivity curves for a special case $g/d=\frac{1}{2}$, and $\rho_2=0$. The ordinate of this figure is

$$\bar{\rho}=\rho/\rho(x=\infty).$$

These curves are W-shaped.

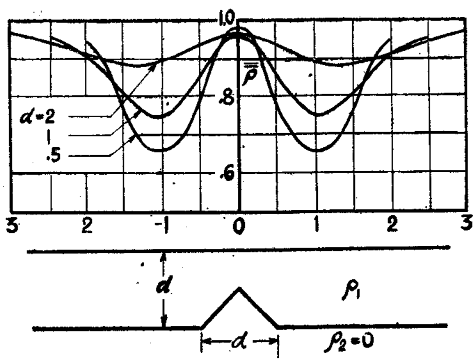

Fig. 10.3.

Fig. 10.4 shows the curves for the non-conducting anticlines. They are inverted V-shaped.

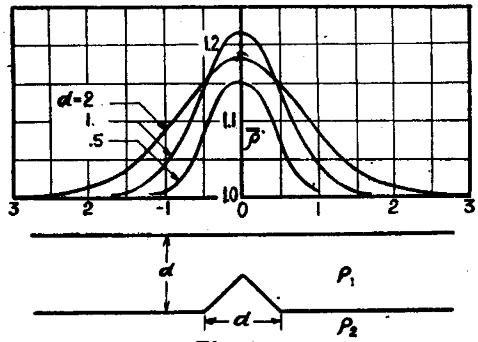

Fig. 10.4.

11. Syncline

As an example for the syncline, we treat the model shown in Fig. 11.1. This is not so important for practice as the anticline described in the former section, but of theoretical interest.

11.1. Theory.

The domain of the z-plane shown in Fig. 11.2 can be transformed to the ς-plane, which is similar to Fig. 10.2 (c), by the following equation:

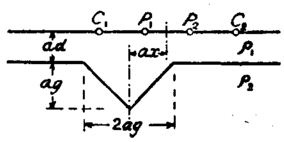

Fig. 11.1.

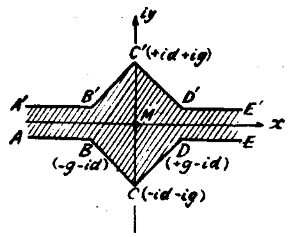

Fig. 11.2.

$$dz = C(\varsigma^2-1)^{-\frac{3}{4}}\left(\varsigma^2-\frac{1}{h^2}\right)^{\frac{1}{4}} d\varsigma. \tag{11.1}$$

Inserting ς of (10.2) into the above equation, and integrating, we get:

$$z = C\frac{1}{\sqrt{2}}\frac{\text{sn}\alpha}{\text{dn}\alpha}\left[2\frac{\text{dn}^3\alpha}{\text{sn}\,\alpha\cdot\text{cn}\,\alpha}w + \Pi(w,d) + i\Pi(w,i\alpha)\right] \tag{11.2}$$

in which the parameter α is related to h by (10.4).

By representing the Π-function by the ϑ-function, z can be written as follows:

$$z = i\frac{2d}{\pi}\left[\frac{d+g}{d}\pi v + \frac{1}{2}\log\frac{\vartheta_0(v-c\,|\,\tau)}{\vartheta_0(v+c\,|\,\tau)} + \frac{i}{2}\log\frac{\vartheta_0(v-ic\,|\,\tau)}{\vartheta_0(v+ic\,|\,\tau)}\right], \tag{11.3}$$

where

$$c=\alpha/(2K), \quad v=w/(2K)$$

and $\tau = i$.

The constant c, which corresponds to the given values of d and g, must be determined from the equation:

$$\frac{\vartheta_1'(c)}{\vartheta_1(c)}+\pi c=\frac{\pi}{2}\,\frac{d+g}{d}\,. \tag{11.4}$$

The relation between x and v'' is as follows:

$$x=\frac{2d}{\pi}\left[-\frac{d+g}{d}\pi v''+\frac{i}{2}\log\frac{\vartheta_0(iv''-c)}{\vartheta_0(iv''+c)}-\frac{1}{2}\log\frac{\vartheta_0(iv''-ic)}{\vartheta_0(iv''+ic)}\right], \tag{11.5}$$

or

$$x=\frac{2d}{\pi}\left[-2\frac{\vartheta_1'(c)}{\vartheta_1(c)}v''+\varphi(v'',c)-\psi(v'',c)\right], \tag{11.6}$$

where φ and ψ are functions, which have been defined by Eq. (10.9).

11.1. Numerical Calculation.

By using the notations in Section 10.2, x can be represented as a function of χ as follows:

$$x=d\,[B_e\chi-T(\chi,\gamma)+L(\chi,\gamma)], \tag{11.7}$$

where

$$B_e=\frac{4}{\pi^2}\,\frac{\vartheta_1'(c)}{\vartheta_1(c)}=\frac{2}{\pi}\left(\frac{d+g}{d}-\frac{2}{\pi}\gamma\right). \tag{11.8}$$

To determine the constant γ, it is convenient to use the following relation:

$$\frac{d+g}{2d}=\frac{\cos\gamma-3q^2\cos 3\gamma+5q^6\cos 5\gamma-\cdots}{\sin\gamma-q^2\sin 3\gamma+q^6\sin 5\gamma-\cdots}+\frac{\gamma}{\pi}. \tag{11.9}$$

The transformations from v to t, consequently from x to s are the same as in the case of anticline (see Section 10.2).

11.3. Resistivity Curves.

In Fig. 11.3, the resistivity curves for the anticlines of the perfect conductor are shown. They are inverted W-shaped, similar to those for the horizontal plates of the "insulator".

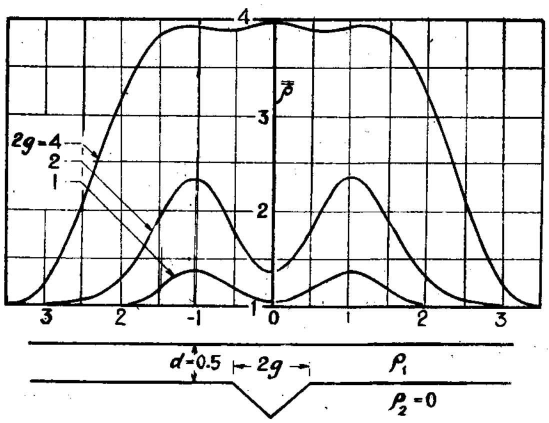

Fig. 11.3.

Fig. 11.4 shows the curves for the insulator; these curves are V-shaped.

It is interesting to compare the curves for the anticline and syncline (see the following table).

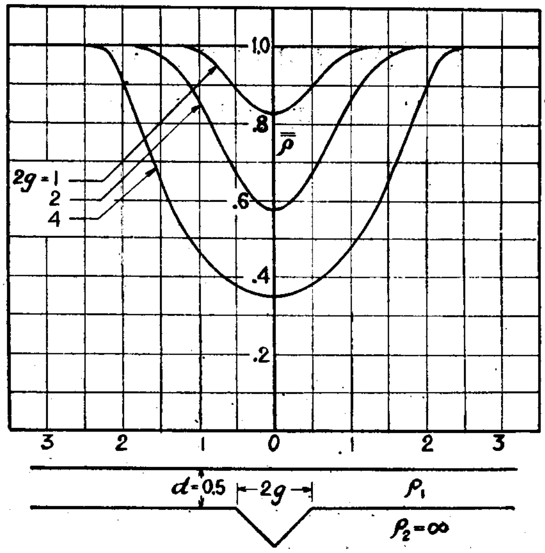

Fig. 11.4.

	Conductor	Non-conductor
Anticline	W	inverted V
Syncline	inverted W	V